Neuropeptides 73 (2019) 49–56

Contents lists available at ScienceDirect

Neuropeptides

journal homepage: www.elsevier.com/locate/npep

Identification and characterization of Prokineticin receptor 2 splicing variant and its modulation in an animal model of Alzheimer's disease

Roberta Lattanzi[a], Daniela Maftei[b], Maria Rosaria Fullone[b], Rossella Miele[b,*]

[a] Dipartimento di Fisiologia e Farmacologia "Vittorio Erspamer", Sapienza Università di Roma, Piazzale Aldo Moro 5, I-00185 Roma, Italy
[b] Dipartimento di Scienze Biochimiche A. Rossi Fanelli, Sapienza Università di Roma, Piazzale Aldo Moro 5, I-00185 Roma, Italy

ARTICLE INFO

Keywords:
Prokineticin
Prokineticin receptor 2
Yeast
Ubiquitin split system
STAT3-Amyloid β

1. Introduction

Prokineticin 2 (PROK2) is a peptide that is widely distributed in the nervous system and influences a variety of brain functions, such as pain, food intake and circadian rhythms (Negri and Lattanzi, 2012; Negri and Ferrara, 2018). PROK2 is able to mediate its signaling through two different G-protein coupled receptors (GPCR), designated prokineticin receptor 1 (PKR1) and prokineticin receptor 2 (PKR2) (Masuda et al., 2002; Soga et al., 2002). They activate multiple intracellular signal-transduction pathways promoting intracellular calcium mobilization (Masuda et al., 2002; Negri and Lattanzi, 2012) by $G\alpha_q$ coupling; they also induce STAT3 activation coupling to $G\alpha_i$ (especially PKR2) and AMPc production by $G\alpha_s$ proteins (Lin et al., 2002; Negri and Ferrara, 2018; Lattanzi et al., 2018). These two receptors have different tissue distributions: PKR1 is expressed in diverse peripheral organs with relatively high levels in the small intestine and lung, whereas PKR2 is predominantly expressed in the central nervous system (Masuda et al., 2002; Soga et al., 2002; Negri and Lattanzi, 2012). Intracerebroventricular (i.c.v.) injection of Amyloid β_{1-42} ($A\beta_{1-42}$) in rat is a well-established animal model of Alzheimer's disease (AD). Previous our studies have reported that following $A\beta_{1-42}$ i.c.v. injection, the levels of PROK2 and its receptors were significantly increased in rat brain hippocampus, suggesting that modulation of the prokineticin system could be a general response to Aβ injury (Severini et al., 2015).

In this work, by PCR amplification from rat hippocampus cDNA, we identified a PKR2 splice variant, which lacking the second exon gives rise to a protein comprising only four transmembrane elements, denominated TM 4–7. So, we have expressed TM 4–7 protein in yeast, explored its dimerization relationship with PKR2 and evaluated its role on PK signaling. We finally evaluated the expression of TM 4–7 in hippocampus of rats $A\beta_{1-42}$ i.c.v. injected and its influence on prokineticin signal transduction.

2. Materials and methods

2.1. Chemical reagents and media

$A\beta_{1-42}$ peptide was purchased from Abcam (Abcam, Cambridge, UK). 1 mg/ml $A\beta_{1-42}$ peptide stock solutions were prepared in Phosphate-Buffered Saline, PBS (0.01 M NaH2PO4, 0.15 M NaCl, pH 7.4) and incubated at 37 °C for 72 h before use. This procedure is known to produce insoluble precipitates and to facilitate markedly the appearance of learning deficits in several tasks (Severini et al., 2015).

Glass beads (425–600 μm, acid-washed), yeast nitrogen base, Ripa buffer, protease inhibitors, fluorescein di-β-D-galactopyranoside, and amino acids were purchased from Sigma. All enzymes used for molecular cloning were from Roche Molecular Biochemicals. The anti-goat IgG antibody conjugated to horseradish peroxidase and nitrocellulose membranes (0.45 μm; Hybond-C Extra) were from Amersham Pharmacia Biotech. The enhanced chemiluminescence detection kit was from Roche Molecular Biochemicals. All other chemicals used for Sodium Dodecyl Sulfate (SDS)-polyacrylamide gel electrophoresis and

Abbreviations: Aβ, amyloid beta; AD, Alzheimer's disease; GFP, green fluorescent protein; GPCR, G protein-coupled receptor; i.c.v., intracerebroventricular; PROK2, Prokineticin 2; PKR1, Prokineticin receptor 1; PKR2, Prokineticin receptor 2; UTR, untranslated sequence; YTH, Yeast Two Hybrid

* Corresponding author.
E-mail address: rossella.miele@uniroma1.it (R. Miele).

https://doi.org/10.1016/j.npep.2018.11.006
Received 17 July 2018; Received in revised form 25 October 2018; Accepted 26 November 2018
Available online 29 November 2018

Western blotting were purchased from Bio-Rad. A goat polyclonal antibody (sc-54316) against the PKR2 amino-terminal region encompassing residues 1–18 was from Santa Cruz Biotechnology, anti-His monoclonal antibodyhorseradish peroxidase conjugate was from Roche Molecular Biochemicals. Mouse anti-STAT3 antibody and mouse anti-pSTAT3 antibody were from Cell Signaling Technology and anti-beta-actin antibody was from Abcam.

2.2. Animals and ethics statement

Experiments were carried out on male adult Sprague-Dawley rats (Charles River, Como, Italy), weighting 280–320 g at the time of surgery. Animals were two/cage housed, under conditions of optimum light, temperature and humidity (12:12 h light/dark cycles, 22 ± 2 °C, 50–60% humidity) with food and water ad libitum.

All procedures involving animal care or treatments were approved by the Animal Care and Use Committee of the Italian Ministry of Health (authorization number: 79/2015-PR) and performed in compliance with the IASP and European Community (E.C.L358/118/12/86) guidelines. All efforts were made to minimize animal suffering and to reduce the number of animals used.

2.3. Surgery and $A\beta_{1-42}$ administration

Under ketamine-xylazine anaesthesia (60 + 10 mg/kg intraperitoneally, i.p.), each rat was surgically implanted with a plastic guide cannula (Linca, Tel-Aviv, Israel), stereotaxically inserted through a skull hole drilled over the left lateral ventricle of the brain (1 mm caudal and 1.8 mm lateral to the bregma). The cannula was screwed into the skull hole and secured to the bone with dental cement. After one week-recovery from surgery, $A\beta_{1-42}$ (1 mg/ml; 5 µl injection volume) or its vehicle (PBS 5 µl injection volume) were i.c.v. injected, in a constant volume of 5 µl in awake rats, using a 10-µl Hamilton syringe fitted with a 26-gauge needle that was inserted through the guide cannula to a depth of 4.2 mm below the external surface of the skull. The needle was left in place for 10 s after the end of the injection to avoid reflux of the solute.

2.4. Yeast strains

The *Saccharomyces cerevisiae* strain used for PKR2 and TM 4–7 co-expression was Cy12946 (MATa FUS1p-HIS3 GPA1Ga $_{i2(5)}$ can1 far1D1442 his3 leu2sst2D2 ste14::trp1::LYS2 ste3D1156 tbt1–1 trp1 ura3), a generous gift from Addison D. Ault (Princeton University, USA). Specifically, Cy12946 expresses a chimeric Gα subunit (GPA1 $G\alpha_{i2(5)}$) in which the carboxyl terminal five amino acids of the yeast Gα subunit, GPA1, are replaced by the carboxyl-terminal five residues of mammalian $G\alpha_{i2}$. The use of GPA1 $G\alpha_{i2(5)}$ required deletion of SST2, which down-regulates the pheromone response pathway by accelerating the GTPase activity of GPA1.

For ubiquitin split assay all yeast strains were generated from NMY63.

To evaluate TM 4–7 activity after PROK2 binding we utilize yeast strains MMY14, MMY23 and MMY28, generous gift of S. Dowell (Glaxo, UK), isogenic except for the Gpa1 gene coding for the yeast G protein α subunit Gpa1p. The three yeast strains harbor genomically integrated mutant versions of Gpa1 coding for mutant Gpa1 proteins in which the last five amino acids are replaced with the homologous mammalian $G\alpha_q$, $G\alpha_{i1/2}$ and $G\alpha_s$ sequences, respectively. Normally, G protein-mediated activation of the pheromone pathway leads to cell cycle arrest; in these strains, instead, deletion of the Far1 gene allows yeast to grow. The Sst2 gene was disrupted to prevent attenuation of G protein signaling, mediated by the GTPase-activating protein Sst2p. The Ste2 gene coding for the yeast α-factor receptor was deleted to prevent competition with heterologous expressed GPCRs for co-expressed G proteins (Brown et al., 2011; Dowell and Brown, 2009).

DNA-mediated yeast transformation was carried out using a lithium acetate method.

2.5. Yeast expression plasmids

The procedure to construct PKR2 pGAD has been previously described (Marsango et al., 2011). cDNA of TM 4–7 splicing variant amplified by PCR, using as template PKR2-pGAD, with oligonucleotides TM 4–7 *BamH*I up and PKR2 dw *EcoR*I was cloned in pYESC3 vector (TM 4–7His). cDNA coding for TM 4–7 fused at C-terminal with His TAG was obtained by digestion of TM 4–7His with *BamH*I and *Pme*I and cloned in p426 vector digested with *BamH*I and *Sma*I (TM 4–7 p426). The p426GPD vector contains the yeast GAPDH (glyceraldehyde-3-phosphate dehydrogenase) promoter and the CYC1 terminator flanking the multiple cloning sites (kind gift of Dr. S. Dowell). The full-length PKR2 receptor and TM 4–7 splicing variant, were PCR-amplified and cloned into the pGAD vector, where it was fused in frame to green fluorescent protein (GFP) cDNA.

The PROK2 cDNAs, cloned downstream the α-factor signal sequence, contained in pPIC9K, were transferred by digestion with *BamH*I-*EcoR*I in p413ADH under the control of the constitutive alcohol dehydrogenase promoter (PROK2-p413). All oligonucleotides used for plasmid constructions are listed in Table 1A.

2.6. Ubiquitin split assay: bait and prey constructs

The full-length PKR2 receptor and TM 4–7 splicing variant, were PCR-amplified with oligonucleotides TM 4–7 NcoI/PKR2 NcoI and PKR2 dw *Hin*dIII cloned into the pBT3 vector, where it was fused in frame to the carboxyl terminal half of ubiquitin (Cub) and a transcription factor (TF) consisting of *Escherichia coli* DNA-binding protein LexA and the activation domain of VP16 from herpes simplex virus. PKR2 cDNA were amplified with oligonucleotides PKR2 BamHI up and PKR2 EcoRI dw and cloned into the pNubG-HA-X vector, pPR3.

2.7. Growth assay

Harvested cells were washed with distilled water and cell suspensions were prepared to give an optical density (OD) at 600 nm of 10. Seven microliters of serial dilutions of cell suspensions (1:10) were spotted on Synthetic Defined (SD) Medium agar plates lacking leucine, tryptophan, adenine and histidine. The plates were incubated at 30 °C.

2.8. Liquid β-galactosidase bioassays

Receptor activation was determined by measuring the induction of β-galactosidase activity under the control of the FUS1 pheromone-inducible promoter. Yeast cells were grown overnight to exponential phase and diluted to give an OD at 600 nm of 0.2 by addition of substrate/lysis solution (1 mM fluorescein di-β-d-galactopyranoside, 0.1 M sodium phosphate, pH 7.3). Yeast cells were incubated for 22 h at 30 °C, and the reactions were stopped by the addition of 20 µl of 1 mM sodium carbonate. Fluorescence was read at an excitation wavelength of 475 nm and an emission wavelength of 520 nm at optimal gain (Dowell and Brown, 2009). Duplicate samples were analyzed and the results shown in the figures are representative of at least three independent experiments.

2.9. Fluorescence imaging

Fluorescence images of cells expressing wild type and TM 4–7 tagged with GFP were captured by using a DAGE cooled CCD camera mounted on an Olympus BH-2 microscope equipped with a DPlanApo100UV 100× objective.

Table 1
Oligonucleotides used in this study.

A.

Oligonucleotide	Sequence
TM4–7 *Bam*HI up	5′- GAG GAT CCA TGG TGT CCA TTC TGG AGA AG-3′
TM4–7 *Nco*I	5′-GAC CAT GGA TGG TGT CCA TTC TGG AGA AG-3′
PKR2 NcoI	5′-GAC CAT GGA TGG CAG CCC AGA ATG G-3′
PKR2 dw EcorI	5′-TTG AAT TCC TTC AGC CTG ATA CAG TCC- 3′
PKR2dwHindIII	5′-GAA AGC TTC TTC AGC CTG ATA CAG TCC- 3′

B.

Gene	Oligonucleotide	Sequence	Annealing temp (°C)	PCR product (bp)	Accession number
PKR2	5′UTRFw	5′-GGC GCC ACC GGC CAG GGA GTG CGT C-3	55	301 TM4–7	XM_006235059
	Ex3Rev	5′-GCC TTG AAC CAG AGC TCT TGG GA G-3		873 PKR2	NM_138978
					CH_473949
SOCS-3	Fw	5′-ACC AGC GCC ACT TCT TCA CA-3′	55	450	NM_053565
	Rev	5′-GTG GAG CAT CAT ACT GGT CC-3′			
GAPDH	Fw	5′-GCG AGA TCC CGC TAA CAT CAA ATG G-3′	60	340	NM_017008
	Rev	5′-GCC ATC CAC AGT CTT CTG AGT GGC-3′			

2.10. Preparation of yeast membranes proteins

Yeast cells from a 1-liter overnight culture (1–2 × 10^7 cells/ml) were collected by centrifugation, and membrane homogenates were prepared using a glass bead method essentially as described previously (Marsango et al., 2011). Membrane preparations (10 µg of protein/sample) were mixed with an equal volume of 2-fold concentrated Laemmli sample buffer (125 mm Tris-HCl, pH 6.8, 20% glycerol, 4% SDS, and 0.01% bromophenol blue) and incubated at 25 °C for 30 min. Proteins were separated on 10% SDS-polyacrylamide gels.

2.11. Western blot assay

After electrophoretic separation the proteins were transferred onto nitrocellulose membrane and blocked in 1% non-fat Milk 1% BSA/Tris-buffered saline with 0.10% Tween-20 (TBS-T pH 7.4) for 1 h at room temperature. Then the membranes were incubated with the appropriate primary antibody at a dilution of 1:1000 overnight at 4 °C in the blocking solution. After extensive washing with TBS-T, the membranes were incubated with anti-mouse IgG, HRP-linked secondary antibody for 1 h at room temperature. Immunoreactive signals were visualized with an enhanced chemiluminescence system.

2.12. RNA purification, reverse transcription and RT-PCR

Total RNA of rats, euthanized 1, 7, 14 and 35 days following $A\beta_{1-42}$ (5 µg) i.c.v. injection, was extracted from brain hippocampus samples using a TRIzol solution Invitrogen (Carlsbad, CA, USA) according to the manufacturer's instructions. RNA yield and purity were determined by spectrophotometry absorption at 260 and 280 nm and 1 µg of mRNA was used to perform reverse transcription (Reverse Transcriptase, Promega) to obtain cDNA that was used as template for RT-PCR and real time-PCR using oligonucleotides showed in Table 1B.

Real time PCR (iCycler; Bio-Rad) was assessed using iQ SYBR Green Supermix (Bio-line, London, U.K.). All the measures were performed in triplicate. The reaction conditions were as follows: 95 °C for 10 min (Polymerase activation); followed by 35 cycles of 95 °C for 30 s, annealing step (Temp. depends on the Tm of primers) for 30 s and elongation at 72 °C for 30 s. The reaction mixture without the cDNA was used as control. The results were quantified using the comparative threshold method. The Ct value of the specific gene of interest was normalized to the Ct value of the endogenous control, glyceralde-hydes-3-phosphate dehydrogenase (GAPDH), and the comparative Ct method (2-ΔΔCt) was then applied using control healthy rats as the reference samples.

For RT-PCR, cDNA was amplified using the Taq DNA Polymerase with specific primers showed in Table 1B under the following conditions: 95 °C for 5 min; 40 cycles of 95 °C for 1 min; annealing for 1 min; extension 72 °C for 1 min; final extension 72 °C for 7 min.

PCR products were separated by electrophoresis on 1.5% agarose gel, visualized with ethidium bromide and analyzed using the Versa Doc 3000 imaging system (Bio-Rad, Milan, Italy).

2.13. Analysis of STAT3 activation

Rat hippocampus was homogenized at 4 °C in 200 µl of Ripa buffer containing protease inhibitors (1% *v*/v). Protein concentrations were determined using the Bradford protein assay. Forty µg of proteins were re-suspended in SDS-bromophenol blue loading buffer with 0.7 M 2-mercaptoethanol. SDS-page gel was analyzed by western blotting assay as described above. The quantification of the signal intensity of the Western blot bands was performed with NIH ImageJ software. The values are expressed as the mean ± SEM of 3 replications for each antibody performed on 3 separate pools.

3. Results

3.1. Cloning of the Prokineticin receptor 2 variant, TM 4–7

In rat and mouse, Pkr2 genes are composed by three exons and two introns. The first exon contains a 5′ untranslated sequence (UTR); the second exon contains a part of the 5′ UTR sequence and a region encoding for the first three transmembrane domains TM1, TM2 and TM3; the third exon encodes for the last transmembrane domains (TM4, TM5, TM6 and TM7) and the 3′ UTR sequence (Fig. 1A). The second intron is located at the TM3 border within the common DRY (Asp-Arg-Tyr) sequence. Intriguingly, the conservation of certain exon-intron boundaries and the relatively high sequence homology between rat and mouse suggests that the Pkr2 genes are evolutionarily related. By computational process (Florea et al., 2005), alternatively spliced mRNA transcript in rat (accession number: EDL80264.1) and in mouse (accession number: XM_011239558.2) for Pkr2 genes were predicted.

To evaluate the presence of PKR2 splicing variants in vivo, we designed specific primers: a forward primer containing a sequence,

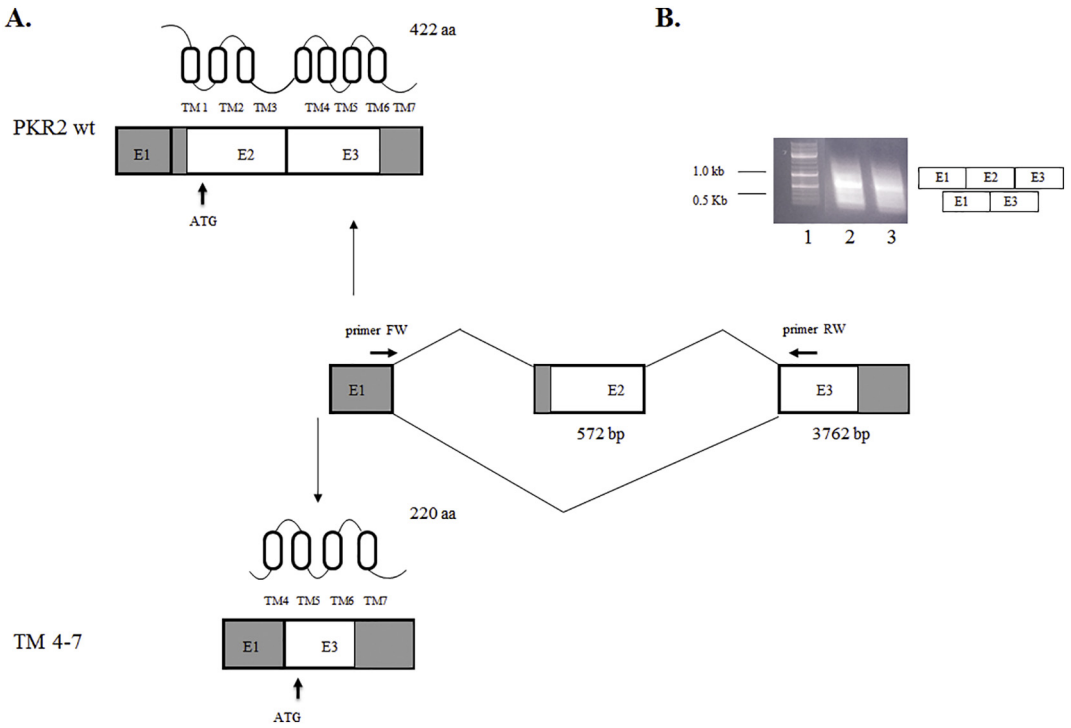

Fig. 1. A. Scheme of alternative splicing of rat Pkr2 gene exons. Exon coding sequences are indicated as white bars and untranslated sequences are shown as gray bars. B. Total RNA harvested from hippocampus (lane 1) and cortex (lane 2) was analyzed for PKR2 expression by RT-PCR. 10% of the PCR products were resolved on 1,5% agarose gel and stained with ethidium bromide. Positions of Standard markers are indicated on the left.

extreme conserved in exon 1, of mouse and rat Pkr2 gene (5′utrFw), and a reverse primer based on a sequence of exon 3 (Ex3Rev). These primers were used to amplify, by PCR assay, the cDNAs obtained by reverse transcription of rat mRNAs hippocampus and cortex. Using rat hippocampus cDNA as template, we obtained two bands: one of about 350 and one of about 900 kb size (Fig.1B). Sequence analysis of fragments indicates that one band encodes for the full-length of PKR2 and one is a splicing variant of PKR2 generated by exon 2 skipping, denominated TM 4–7. The TM 4–7 splicing variant containing only TM4, TM5, TM6 and TM7 is a receptor that lacks important sequences that may be crucial for the recognition of ligand and for Gα coupling.

3.2. Physical association of TM 4–7 with PKR2

Mutant receptor was assessed for its ability to dimerize with PKR2 full-length. TM 4–7 terminal tagged His (TM 4–7His) was expressed with untagged PKR2 full sequence (PKR2 pGAD) in yeast Cy12946. The receptors were immunoprecipitated with the anti-His antibody, subjected to SDS–page, and immuno-detected using a commercial polyclonal antibody raised against a peptide corresponding to the amino-terminal 18-amino acids of PKR2, which does not recognize the TM 4–7 receptor. As seen in Fig. 2A, the anti-His immunoprecipitated detection with the His antibody revealed the presence of the heterodimer TM 4–7/PKR2, with a molecular weight of 90 kDa, and of the dimer TM 4–7/TM 4–7 with a molecular weight of 45 kDa.

Detection of the anti-His immunoprecipitate with the PKR2 antibody (Fig. 2B), permitted to visualize only one band corresponding to the heterodimer TM 4–7/PKR2.

The results were confirmed by in vivo experiments using split-Ubiquitin Yeast Two hybrid system (Nakamura et al., 2013). Upon in vivo protein-protein interaction, the reconstituted ubiquitin leads to cleavage and release of LexA-VP16 by ubiquitin-specific proteases; therefore, the protein interaction may be detected via the transcription activation of the reporter genes (ADE, HIS3, and lacZ). To test the viability of split-ubiquitin–based reporter gene assays for detecting

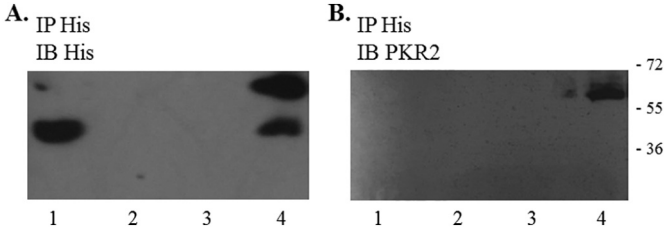

Fig. 2. Detection of TM 4–7 dimerization with PKR2 receptor in yeast strain by immunoprecipitation. Membranes proteins from yeast immunoprecipitated using Ni-NTA His bind resin were resolved by SDS-page. The immunoblots were probed with anti-His (panel A) and anti-PKR2 (panel B) antibodies. Membranes proteins from CyCp yeast strain expressing: Lane 1, TM 4–7 splicing variant; Lane 2, CyCp; Lane 3, empty; Lane 4, PKR2 and TM 4–7 splicing variant.

PKR2 dimers, we first analyzed the homodimerization of PKR2 receptor in the NMY62 yeast strain. In NMY62 strain, were expressed two chimeric proteins: PKR2-NubG and PKR2-Cub-lexA.

PKR2-NubG was obtained fusing the N-terminal moiety of split-ubiquitin, containing an I13G mutation (NubG), with PKR2 using the original pPR3-C vector (prey). PKR2-Cub-lexA was obtained fusing the C-terminal ubiquitin moiety, linked to an artificial transcription factor (Cub-LexA-VP16) (Nakamura et al., 2013), to the C-termini of PKR2 receptors by using pBT3-C (bait) split-ubiquitin vector.

In particular, in yeasts coexpressing PKR2-NubG and/or PKR2-Cub-lexA separately, we measured the β-galactosidase activities (Fig. 3A). To validate this result, yeast strains were also grown on adenine/histidine-deficient media (Fig. 3B). The results obtained indicate that the split-ubiquitin-based approach could detect the homodimerization of PKR2 receptors.

Then, we replaced a cDNA coding for full-length PKR2 with a cDNA coding for the splicing variant TM 4–7 in pBT3-C (Fig. 3). These results were coincident with immunoprecipitation experiments (Fig. 2) showing TM 4–7 receptor ability to form heterodimers with full-length PKR2.

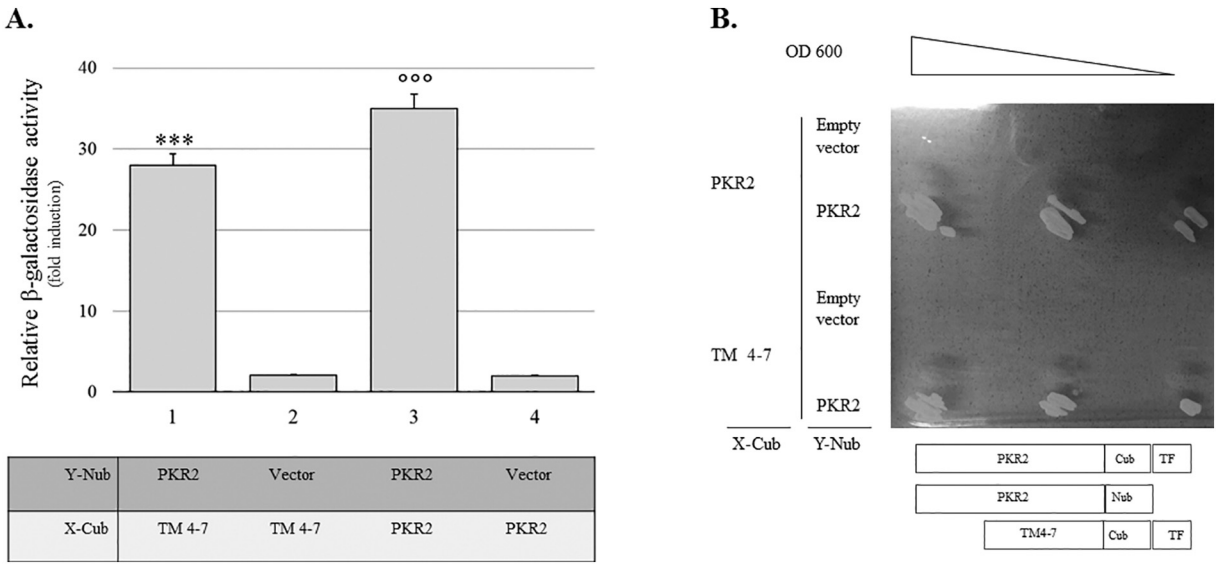

Fig. 3. Detection of TM 4–7 dimerization with PKR2 by ubiquitin split assay. Yeast Cells expressing different combinations of Cub and NubG fusion proteins were analyzed by: A. Quantitative β-galactosidase assay. B. Growth assay: each cells colture was spotted in serial 10-fold dilutions on SD-Leu, Trp, Ade and His dropout plate. The control prey plasmid was pBT3c vector. Data are expressed as mean of five independent experiments ± SEM. Data were determined as significantly different from response induced in yeast transfected with only one vector. Student's *t*-test was used for statistical evaluation: ***$p < 0.001$ PKR2/TM 4–7 vs TM 4–7; °°°$p < 0.001$ PKR2/PKR2 vs PKR2.

3.3. Yeast cell surface expression of TM 4–7 Prokineticin receptor variant

Because certain mutations in GPCR impair stability of receptors, it was necessary to determine whether TM 4–7, being a receptor fragment, trafficked normally to the plasma membrane. By fluorescence microscopy we evidenced that GFP-tagged TM 4–7, like GFP-tagged PKR2 wt receptor, localized on the plasma membrane (Fig. 4).

3.4. Functional expression of Prokineticin receptors and ligands in yeast

To investigate the activation mechanism of TM 4–7 splicing variant by PROK2, we expressed TM 4–7, modified at the intracellular C-terminus by incorporation of the His-tag, in three different yeast strains carrying chimeras of 1–467 amino acid residues of yeast Gpa1 followed by the last five amino acids of human $G\alpha_q$ (MMY14), $G\alpha_i$ (MMY23), and $G\alpha_s$ (MMY28) (Fig. 5).

All yeast strains used in this study have been engineered so that receptor signaling leads to activation of the yeast-mating pathway resulting in the expression of a PFUS1-HIS3 and PFUS1-β-galactosidase reporter gene (Dowell and Brown, 2009; Brown et al., 2011). This system permits to evaluate the prokineticin receptors activation (Lattanzi et al., 2018). Set of three yeast strains were obtained and denominated MMY14 TM4–7, MMY28 TM 4–7, and MMY23 TM 4–7 respectively. Whole-cell extracts of yeast strains were analyzed by Western blot using an antibody against His-Tag and we demonstrated that the expression levels of TM 4–7 were comparable in different yeast strains (Fig. 5A). Since it is difficult for large peptides to penetrate the yeast cell wall, we decided to express PROK2 as an autocrine molecule. We transformed each yeast strain with PROK2-p413 plasmid obtaining a set of three yeast strains. Once assessed the expression level of TM 4–7, we performed a β-galactosidase assay using a fluorescein-containing galactopyranoside analog that allowed the quantification of the receptor activation by the measurement of the fluorescence signal at 530 nm.

The difference in β-galactosidase activity between cells expressing or not PROK2, evidenced that TM 4–7 can be expressed in functionally active and G protein-selective conformations to activate an endogenous MAPK pathway in yeast cells (Fig. 5B). Data are presented as fold induction with respect to control yeast expressing only ligand that exhibited negligible FUS1-lacZ activation. Co-expression of TM 4–7 with PROK2 clearly showed that the splicing variant coupled to $G\alpha_q$, and $G\alpha_s$ but not Gαi (Fig. 5C). Relative maximal FUS1-lacZ was calculated respect to values obtained with PKR2 (Lattanzi et al., 2018).

We analyzed if co-expression of TM 4–7 with PKR2 wt could modulate activity of full length receptor evaluating β-galactosidase activity of yeast strain Cy12946 transformed with TM 4–7His, PKR2 pGAD and

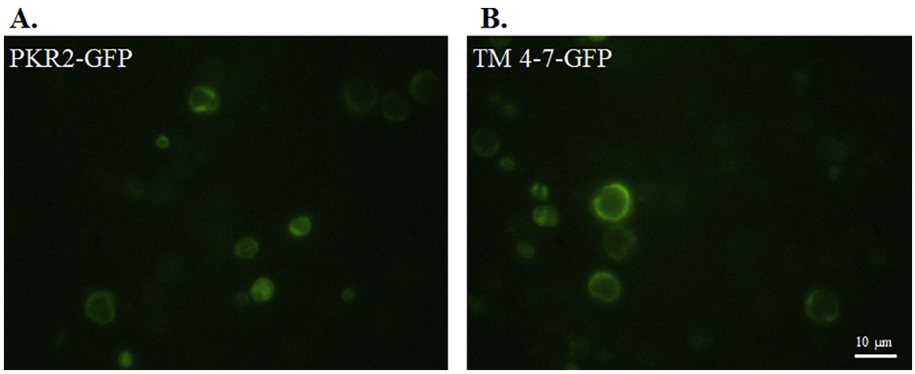

Fig. 4. Fluorescence confocal microscopy analysis showing plasma membrane localization of TM 4–7 and PKR2. Scale bar 10 µm.

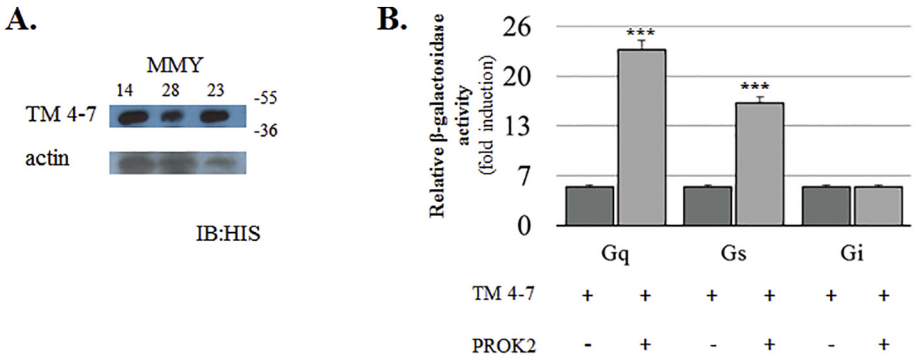

C.

PROK2			
Receptors	**Relative maximal FUS1-LacZ**	**Relative maximal FUS1-LacZ**	**Relative maximal FUS1-LacZ**
PKR2 wt	**1.00+/- 0.03**	**1.00+/-0.05**	**1.00+/-0.04**
TM 4-7	0.84+/-0.01	0.58+/-0.01	N.D
	Gαq MMY14	Gαs MMY28	Gαi MMY23

Fig. 5. TM 4–7 induces preferentially $G\alpha_q$, $G\alpha_s$, but not $G\alpha_i$, coupling. (A) Expression of Prokineticin receptors. Cells extract expressing PKR2-HIS and TM 4–7HIS were resolved by SDS-page. Western blots were probed with an anti-his-antibody, stripped and reprobed with an anti-beta actin antibody as a loading contr. (B) Yeast strains MMY14, MMY28, and MMY23 expressing the receptor PKR2 (*dark gray bar*) or the receptor TM 4–7 and the ligand PK2 (*light gray bar*). The resulting fluorescence activity was measured at 485 nm excitation, 530 nm emission. Data from each experiment are presented as a relative β-galactosidase activity (fold induction rather than absolute values). Data are presented as fold induction with respect to control yeast expressing only ligand that exhibited negligible *FUS1-lacZ* activation. Data are mean five independent experiments ± SEM. Data were determined as significantly different from the non peptide response using Student's *t*-test where ***p < 0.001. (C) β-galactosidase activity in yeast strains MMY14, MMY28 and MMY23 expressing $G\alpha_q$, $G\alpha_s$ and $G\alpha_i$ proteins respectively, and the receptor TM 4–7. Relative maximal FUS1-lacZ induction was calculated with respect to wild type PKR2 receptors when induced with the highest concentration of ligands. Data are mean five independent experiments ± SEM.

PROK2-p413. The results obtained demonstrated a drastic reduction of $G\alpha_i$ activation (about 45%).

3.5. Up-regulation of TM 4–7 following Aβ insult

In hippocampus from adult rats we evaluated, by RT-PCR analysis, TM 4–7 and PKR2 mRNA levels 7, 14 and 35 days after $A\beta_{1-42}$ i.c.v. injection.

Time-course analysis (7, 14, 35 days) indicated that TM 4–7 mRNA was progressively increased 7, 14 and 35 days after $A\beta_{1-42}$ injection, whereas PKR2 mRNA showed a biphasic pattern of expression, with an increase at 7 and 14 days followed by a decrease at 35 days when its levels appeared overlapped to that of controls (Fig. 6).

3.6. STAT3 activation and Socs-3 gene expression in rat hippocampus after Aβ treatment

We evaluated, by western blotting experiments, the STAT3 phosphorylation in rat brain hippocampus 14 and 35 days after $A\beta_{1-42}$ i.c.v. injection. Rat hippocampal tissues were homogenized, and the lysates were gel transferred on nitrocellulose membrane and incubated with STAT3 and p-STAT3 antibodies.

In rat hippocampus, there was a STAT3 phosphorylation significantly higher respect to control animals only 14 days after $A\beta_{1-42}$ treatment; this activation was not abolished by pretreatment with the PKRs antagonist PC1 (Fig. 7A). Conversely, 35 days after $A\beta_{1-42}$ injection the p-STAT3 levels were lower than that observed in control animals (Fig. 7A).

STAT3 regulates transcription of Socs-3 gene (Kershaw et al., 2013). An increase in SOCS-3 mRNA levels was observed in hippocampus of rats scarified 14 days after $A\beta_{1-42}$ administration, respect to control animals (Fig. 7B, C). 35 days after $A\beta_{1-42}$ injection the SOCS-3 mRNA levels were lower than that observed in controls (Fig. 7B, C).

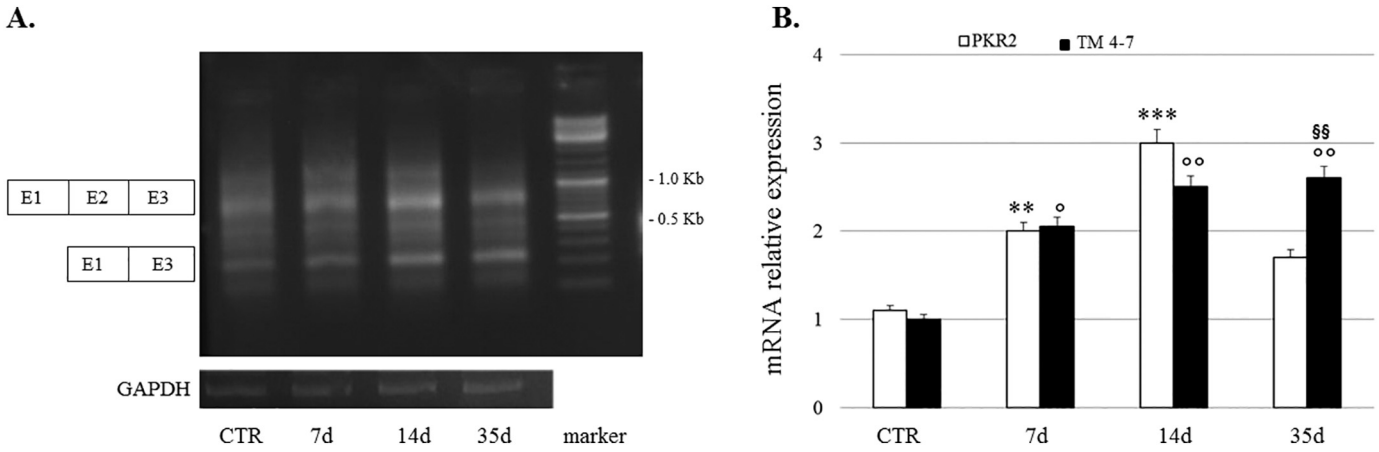

Fig. 6. Expression of TM 4–7 and PKR2 following Aβ insult. A. Analysis of PCR amplicons by gel electrophoresis. The left lane indicates the molecular marker. B. Ratio between TM 4–7 and PKR2 mRNA was analyzed by NIH ImageJ software. The mRNA expression levels were expressed in relation to GAPDH. Data represent means (± SEM) from at least 4 independent experiments and the statistically significant differences were calculated by Student's *t*-test **p < 0.01, ***p < 0.001 vs CTR (PKR2); °p < 0.05, °°p < 0.01 vs CTR (TM 4–7); §§p < 0.01 TM 4–7 35d vs PKR2 35d.

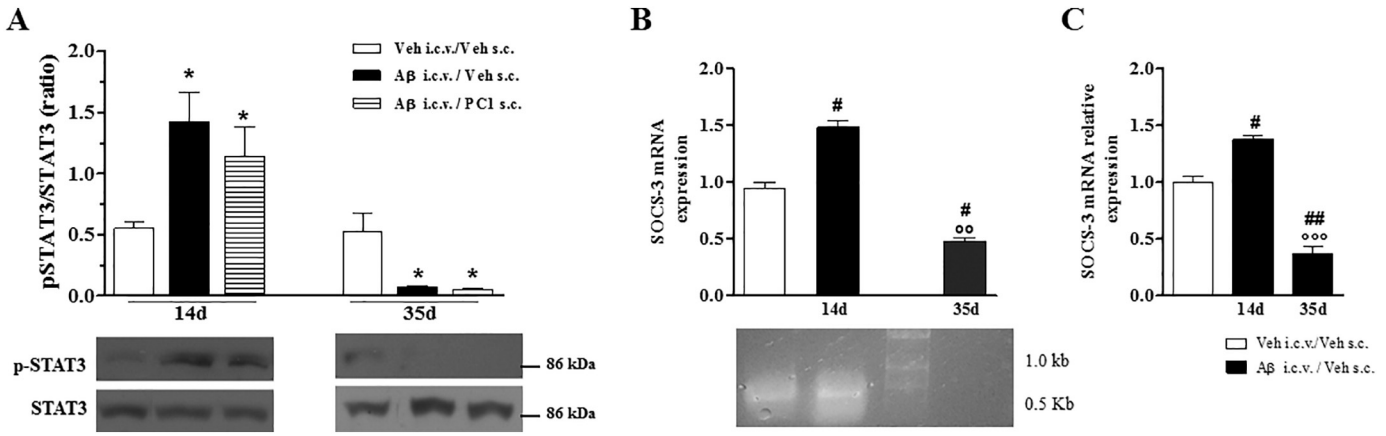

Fig. 7. STAT3 activation and SOCS-3 expression 14 and 35 days after Aβ treatment. A. Representative Western blot analysis showing phospho-STAT3 (p-STAT3) and STAT3 protein amounts 14 and 35 days after Aβ insult. Data are express as mean ± SEM. Statistical analyses were performed using Student's t-test where *p < 0.05 vs Veh i.c.v./Veh s.c. B, C. RT-PCR and Real Time RT-PCR analysis showing SOCS-3 mRNA levels in hippocampus of rat 14 and 35 days after $A\beta_{1-42}$ injection. The mRNA expression levels were expressed in relation to GAPDH. Data are express as mean ± SEM. Statistical analyses were performed using Student's t-test where $^{\#}p < 0.05$, $^{\#\#}p < 0.01$ vs Veh i.c.v./Veh s.c.; °p < 0.01, °°°p < 0.001 vs Aβ i.c.v./Veh s.c. 14d.

4. Discussion

Alternative splicing is a ubiquitous regulatory mechanism of gene expression that allows generation of more than one unique mRNA species from a single gene through mechanisms that include the removal of specific exons, exon skipping, a choice between mutually exclusive exons and the use of alternative splice sites. Strong splice sites with consensus sequences are always recognized by the spliceosome machinery and determine a constitutive splicing. Weak splice sites differ from consensus sequences, and their recognition by the spliceosome is highly dependent by the presence of cis-acting sequences and the cellular context, such as splicing-factor expression levels (Chen and Manley, 2009). Alternative splicing of GPCR increases receptor isoforms and signal options in health and disease (Markovic and Challiss, 2009; Wise, 2012). Sequence analysis of the mouse and rat genome indicates that Pkr2 gene consists of three exons and two introns. Also mouse Pkr1 gene is composed by three exons although in the past was suggested to consist only of two exons (Parker et al., 2000). The positions and sequences of the splice donor and acceptor sites and the length of exons are exactly the same for mouse and rat Pkr2 genes. In contrast, the length of the introns considerably varies as well as their sequences.

By informatic study (Florea et al., 2005) it was possible to predict the splicing variant of murine and rat Pkr2 gene. Given the differences in the genomic intron sequences, it is not obvious that all the splice variants present in one species also occur in other species. The creation of PKR2 knock out mice, by transposon insertion inside the intron 2, allowed the authors to found two transcripts: one, containing exon 1 and exon 2, due to the block of transcription for the presence of the transposon, and one containing exon 1 and 3, due to excision of exon 2 and transposon (Prosser et al., 2007).

This result can be explained, in the light of our data, as the first evidence of the presence of alternative PKR2 splicing transcripts in vivo.

We identified the PKR2 splicing variant, TM 4–7, in rat hippocampus whereas it was undetectable in rat cortex. Moreover, in this study we characterized the truncated PKR2 receptor by expression in yeast heterologous system. We have previously shown that PKR2 forms active dimers in physiologically relevant cell types and in heterologous expression system (Marsango et al., 2011; Sposini et al., 2015). We evidenced the capacity of TM 4–7 receptor to form heterodimers with PKR2 receptor by immunoprecipitation assay. To confirm in vivo immunoprecipitation data we used the split-ubiquitin membrane yeast two hybrid technology. Unlike the Yeast Two Hybrid (YTH), the split-ubiquitin membrane YTH is not limited to the analysis of soluble proteins thus offers the opportunity to identify membrane protein interactions as they take place in their natural setting (Nakamura et al., 2013). TM 4–7 is still able to interact with PKR2 according to our previous data showing that PKR2 protomers involve TM4 and TM5 (Sposini et al., 2015). To investigate if TM 4–7 is activated by PROK2, we expressed the mutant receptor in yeast strains (Dowell and Brown, 2009; Brown et al., 2011) that only differ in the nature of the Gα protein subunit present. The splicing variant partially retained signal transduction activity by $G\alpha_s$ and $G\alpha_q$ coupling but it completely lost activity in the presence of $G\alpha_i$. Co-transfection of TM 4–7 in cells expressing PKR2 negatively modulates $G\alpha_i$-induced signal responses.

In the past (Sposini et al., 2015), we have created a PKR2 variant, TM 1–5, obtained deleting the last two transmembrane domains and the carboxyl-terminal tail, that is still able to form dimers with PKR2. TM 1–5 alone does not exert in vitro signal transduction activity, however, when it is co-expressed with the PKR2, it markedly exhibits ligand-induced calcium responses. These our data are confirmed in a study conducted in patients with precocious puberty which overexpress the TM 1–5 PKR2 variant (Fukami et al., 2017). Truncated receptors, TM 1–5 and TM 4–7, which share only the region spanning TM4 and TM5 crucial for the dimer formation, are both able to interact with PKR2 but they modulate the PKR2 receptor activity in a different fashion.

Data from our laboratory, showed that, in the animal model of AD induced by $A\beta_{1-42}$ i.c.v. injection in rat (Selkoe, 2001; Rubio-Perez and Morillas-Ruiz, 2012) there was a significant increase in PKR2 mRNA levels not corresponding to PKR2 protein levels increase, detected by an antibody against the PKR2 N-terminal region (data in publication). It has been demonstrated that, in AD, there is a modulation of alternative splicing of genes, notoriously involved in this pathology, like the β-amyloid precursor protein, TAU, and apolipoprotein E (Love et al., 2015). For this reason we decided to investigate if TM 4–7 receptor isoform could be regulated in the animal model of AD, induced by $A\beta_{1-42}$ i.c.v. injection in rat and we found that TM 4–7 receptor isoform is strongly up- regulated and the expression ratio between the PKR2 splicing variant and the PKR2 long form significantly and progressive increased 14 and 35 days after Aβ insult in rat hippocampus.

So, we evaluated if TM 4–7 increased levels could induce an alteration in $G\alpha_i$-mediated response after PROK2 binding. As reported in literature, PROK2 is able to induce STAT3 phosphorylation (Qu et al., 2012; Xin et al., 2013) and we demonstrated that, in rat dorsal root ganglia explants, PROK2 is able to induce STAT3 activation through $G\alpha_i$ because it is abolished by pertussis toxin pretreatment (Lattanzi et al., 2018).

In rat hippocampus, 14 days after Aβ administration there was a significant p-STAT3 increase respect to hippocampus from control animals. Despite the presence of high levels of PROK2 (data in publication), STAT3 phosphorilation did not involve PKR2 activation because it was not abolished by PC1 (the PKR antagonist) pretreatment (Balboni et al., 2008; Lattanzi et al., 2014). This suggested us that the presence of high levels of TM 4–7 prevented PROK2-induced STAT3 phosphorilation. Conversely, 35 days after Aβ treatment was not possible to determine STAT3 activation, according to data showing that Aβ chronic stimulation there are very low p-STAT3 levels in hippocampal neurons (Chiba et al., 2009). These data were confirmed by suppressor of cytokine signaling (SOCS-3) expression analysis. SOCS proteins are the key anti-inflammatory regulators of JAK–STAT pathways and their expression is up-regulated after STAT activation (Kershaw et al., 2013). Notably, high levels of SOCS3 are correlated with Aβ deposition (Cianciulli et al., 2017). Our data indicate that SOCS3 levels are elevated 14 days after $A\beta_{1-42}$ injection but not 35 days after Aβ insult correlating with STAT3 activation.

TM 4–7 could generate functionally active receptors by heterodimerization with PKR2, like other truncated splice variants of GPCR (Markovik and Challiss, 2009; Wise, 2012; Xu et al., 2013), or could form active homodimers as described for chemokine receptors (Ling et al., 1999).

TM 4–7, both as heterodimer and homodimer, shows different functional characteristics respect to PKR2 dimers. The different TM 4–7 receptor distribution, in physiological and in pathologic conditions, suggests a versatile way of regulation of brain functions which adds another layer of complexity onto the Prokineticin system.

References

Balboni, G., Lazzari, I., Trapella, C., Negri, L., Lattanzi, R., Giannini, E., Nicotra, A., Melchiorri, P., Visentin, S., De Nuccio, C., Salvadori, S., 2008. Triazine compounds as antagonists at Bv8-prokineticin receptors. J. Med. Chem. 51, 7635–7639. https://doi.org/10.1021/jm800854e.

Brown, A.J., Daniels, D.A., Kassim, M., Brown, S., Haslam, C.P., Terrell, V.R., Brown, J., Nichols, P.L., Staton, P.C., Wise, A., Dowell, S.J., 2011. Pharmacology of GPR55 in yeast and identification of GSK494581A as a mixed-activity glycine transporter subtype 1 inhibitor and GPR55 agonist. J. Pharmacol. Exp. Ther. 337, 236–246. https://doi.org/10.1124/jpet.110.172650.

Chen, M., Manley, J.L., 2009. Mechanisms of alternative splicing regulation: insights from molecular and genomics approaches. Nat. Rev. Mol. Cell Biol. 10, 741–754. https://doi.org/10.1038/nrm2777.

Chiba, T., Yamada, M., Sasabe, J., Terashita, K., Shimoda, M., Matsuoka, M., Aiso, S., 2009. Amyloid-β causes memory impairment by disturbing the JAK2/STAT3 axis in hippocampal neurons. Mol. Psychiatry 14, 206–222. https://doi.org/10.1038/mp.2008.105.

Cianciulli, A., Calvello, R., Porro, C., Trotta, T., Panaro, M.A., 2017. Understanding the role of SOCS signaling in neurodegenerative diseases: current and emerging concepts. Cytokine Growth Factor Rev. 37, 67–79. https://doi.org/10.1016/j.cytogfr.2017.07.005.

Dowell, S.J., Brown, A.J., 2009. Yeast assays for G protein-coupled receptors. Methods Mol. Biol. 552, 213–229. https://doi.org/10.1007/978-1-60327-317-6_15.

Florea, L., Di Francesco, V., Miller, J., Turner, R., Yao, A., Harris, M., Walenz, B., Mobarry, C., Merkulov, G.V., Charlab, R., Dew, I., Deng, Z., Istrail, S., Li, P., Sutton, G., 2005. Gene and alternative splicing annotation with AIR. Genome Res. 1, 54–66. https://doi.org/10.1101/gr.2889405.

Fukami, M., Suzuki, E., Izumi, Y., Torii, T., Narumi, S., Igarashi, M., Miyado, M., Katsumi, M., Fujisawa, Y., Nakabayashi, K., Hata, K., Umezawa, A., Matsubara, Y., Yamauchi, J., Ogata, T., 2017. Paradoxical gain-of-function mutant of the G-protein-coupled receptor PROKR2 promotes early puberty. J. Cell. Mol. Med. 21 (10), 2623–2626. https://doi.org/10.1111/jcmm.13146.

Kershaw, N.J., Murphy, J.M., Lucet, I.S., Nicola, N.A., Babon, J.J., 2013. Regulation of Janus kinases by SOCS proteins. Biochem. Soc. Trans. 41, 1042–1047. https://doi.org/10.1042/BST20130077.

Lattanzi, R., Congiu, C., Onnis, V., Deplano, A., Salvadori, S., Marconi, V., Maftei, D., Francioso, A., Ambrosio, C., Casella, I., Costa, T., Caltabiano, G., Matsoukas, M.T., Balboni, G., Negri, L., 2014. Halogenated triazinediones behave as antagonists of PKR1: in-vitro and in-vivo pharmacological characterization. Int. J. Pharm. Sci. Res. 5 (11), 5066–5074. https://doi.org/10.13040/IJPSR.0975-8232.6(3).1033-42.

Lattanzi, L., Maftei, D., Negri, L., Fusco, I., Miele, R., 2018. PK2β ligand, a splice variant of prokineticin 2, is able to modulate and drive signaling through PKR1 receptor. Neuropeptides 2018https://doi.org/10.1016/j.npep.2018.06.005. (In press).

Lin, D.C.H., Bullock, C.M., Ehlert, F.J., Chen, J.L., Tian, H., Zhou, Q.Y., 2002. Identification and molecular characterization of two closely related G protein-coupled receptors activated by prokineticins/endocrine gland vascular endothelial growth factor. J. Biol. Chem. 277, 19276–19280. https://doi.org/10.1074/jbc.M202139200.

Ling, K., Wang, P., Zhao, J., Wu, Y.L., Cheng, Z.J., Wu, G.X., Hu, W., Ma, L., Pei, G., 1999. Five-transmembrane domains appear sufficient for a G protein-coupled receptor: functional five-transmembrane domain chemokine receptors. Proc. Natl. Acad. Sci. U. S. A. 96, 7922–7927. https://doi.org/10.1073/pnas.96.14.7922.

Love, J.E., Hayden, E.J., Rohn, T.T., 2015. Alternative splicing in Alzheimer's disease. J. Parkinsons Dis. Alzheimers Dis. 2 (2), 6. https://doi.org/10.13188/2376-922X.1000010.

Markovic, D., Challiss, R.A., 2009. Alternative splicing of G protein-coupled receptors: physiology and pathophysiology. Cell. Mol. Life Sci. 66, 3337–3352. https://doi.org/10.1007/s00018-009-0093-4.

Marsango, S., Bonaccorsi Di Patti, M.C., Barra, D., Miele, R., 2011. Evidence that prokineticin receptor 2 exists as a dimer in vivo. Cell. Mol. Life Sci. 68, 2919–2929. https://doi.org/10.1007/s00018-010-0601-6.

Masuda, Y., Takatsu, Y., Terao, Y., Kumano, S., Ishibashi, Y., Suenaga, M., Abe, M., Fukusumi, S., Watanabe, T., Shintani, Y., Yamada, T., Hinuma, S., Inatomi, N., Ohtaki, T., Onda, H., Fujino, M., 2002. Isolation and identification of EG-VEGF/prokineticins as cognate ligands for two orphan G-protein-coupled receptors. Biochem. Biophys. Res. Commun. 293, 396–402. https://doi.org/10.1016/S0006-291X(02)00239-5.

Nakamura, Y., Ishii, J., Kondo, A., 2013. Rapid, facile detection of heterodimer Partners for target human G-protein-coupled receptors using a modified split-ubiquitin membrane yeast two-hybrid system. PLoS One 8 (6), e66793. https://doi.org/10.1371/journal.pone.0066793. (Print 2013).

Negri, L., Ferrara, N., 2018. The prokineticins: neuromodulators and mediators of inflammation and myeloid cell-dependent angiogenesis. Phys. Rev. 98 (2), 1055–1082. https://doi.org/10.1152/physrev.00012.2017.

Negri, L., Lattanzi, R., 2012. Bv8/PROK2 and prokineticin receptors: drugs able nociceptive system. Curr. Opin. Pharmacol. 12, 62–66. https://doi.org/10.1016/j.coph.2011.10.023.

Parker, R., Liu, M., Eyre, H.J., Copeland, N.G., Gilbert, D.J., Crawford, J., Sutherland, G.R., Jenkins, N.A., Herzog, H., 2000. Y-receptor-like genes GPR72 and GPR73: molecular cloning, genomic organisation and assignment to human chromosome 11q21.1 and 2p14 and mouse chromosome 9 and 6. Biochim. Biophys. Acta 1491, 369–375. https://doi.org/10.1016/S0167-4781(00)00023-3.

Prosser, H.M., Bradley, A., Chesham, J.E., Ebling, F.J., Hastings, M.H., Maywood, E.S., 2007. Prokineticin receptor 2 (Prokr2) is essential for the regulation of circadian behavior by the suprachiasmatic nuclei. Proc. Natl. Acad. Sci. U. S. A. 104, 648–653. https://doi.org/10.1073/pnas.0606884104.

Qu, X., Zhuang, G., Yu, L., Meng, G., Ferrara, N., 2012. Induction of Bv8 expression by granulocyte colony-stimulating factor in CD11b+Gr1+ cells: key role of Stat3 signaling. J. Biol. Chem. 287, 19574–19584. https://doi.org/10.1074/jbc.M111.326801.

Rubio-Perez, J.M., Morillas-Ruiz, J.M., 2012. A review: inflammatory process in Alzheimer's disease, role of cytokines. Sci. World J. 2012. https://doi.org/10.1100/2012/756357.

Selkoe, D.J., 2001. Alzheimer's disease results from the cerebral accumulation and cytotoxicity of amyloid beta-protein. J. Alzheimers Dis. 3 (1), 75–80. https://doi.org/10.3233/JAD-2001-3111.

Severini, C., Lattanzi, R., Maftei, D., Marconi, V., Ciotti, M.T., Petrocchi Passeri, P., Florenzano, F., Del Duca, E., Caioli, S., Zona, C., Balboni, G., Salvadori, S., Nisticò, R., Negri, L., 2015. Bv8/prokineticin 2 is involved in Aβ-induced neurotoxicity. Sci. Rep. 19 (5), 15301. https://doi.org/10.1038/srep1530.

Soga, T., Matsumoto, S., Oda, T., Saito, T., Hiyama, H., Takasaki, J., Kamohara, M., Ohishi, T., Matsushime, H., Furuichi, K., 2002. Molecular cloning and characterization of prokineticin receptors. Biochem. Biophys. Acta 1579, 173–179. https://doi.org/10.1016/S0167-4781(02)00546-8.

Sposini, S., Caltabiano, G., Hanyaloglu, A.C., Miele, R., 2015. Identification of transmembrane domains that regulate spatial arrangements and activity of prokineticin receptor 2 dimers. Mol. Cell. Endocrinol. 399, 362–372. https://doi.org/10.1016/j.mce.2014.10.024.

Wise, H., 2012. The roles played by highly truncated splice variants of G protein-coupled receptors. J. Mol. Signal. 7, 13. https://doi.org/10.1186/1750-2187-7-13.

Xin, H., Lu, R., Lee, H., Zhang, W., Zhang, C., Deng, J., Liu, Y., Shen, S., Wagner, K.U., Forman, S., et al., 2013. G-protein-coupled receptor agonist Bv8/prokineticin-2 and STAT3 protein form a feed-forward loop in both normal and malignant myeloid cells. J. Biol. Chem. 288, 13842–13849. https://doi.org/10.1074/jbc.M113.450049.

Xu, J., Xu, M., Brown, T., Rossi, G.C., Hurd, Y.L., Inturrisi, C.E., Pasternak, G.W., Pan, Y.X., 2013. Stabilization of the μ-opioid receptor by truncated single transmembrane splice variants through a chaperone-like action. J. Biol. Chem. 288, 21211–21227. https://doi.org/10.1074/jbc.M113.458687.